J Mater Sci (2011) 46:1646–1654
DOI 10.1007/s10853-010-4981-7

Photocatalytic activity of polypyrrole/TiO_2 nanocomposites under visible and UV light

Qingzhi Luo · Xueyan Li · Desong Wang · Yanhong Wang · Jing An

Received: 21 August 2010 / Accepted: 5 October 2010 / Published online: 20 October 2010

Abstract A series of polypyrrole (PPy)/titanium dioxide (TiO_2) nanocomposites were prepared in different polymerization conditions by 'in situ' chemical oxidative polymerization. The nanocomposites were characterized by transmission electron microscopy (TEM), Fourier transform infrared spectra (FT-IR), X-ray photoelectron spectroscopy spectra (XPS), and UV–Vis diffuse reflectance spectra. The photocatalytic degradation of methyl orange (MO) was chosen as a model reaction to evaluate the photocatalytic activities of TiO_2/PPy catalysts. The results show that a strong interaction exists at the interface between TiO_2 and PPy, the deposition of PPy on TiO_2 nanoparticles can alleviate their agglomeration, PPy/TiO_2 nanocomposites show stronger absorbance than neat TiO_2 under the whole range of visible light. The obtained PPy/TiO_2 nanocomposites exhibit significantly higher photocatalytic activity than the neat TiO_2 on the degradation of MO aqueous solution under visible and UV light illumination. The reasons for improving the photocatalytic activity were also discussed.

Introduction

Nanoparticulate TiO_2 has attracted much attention in last score years not only for its effectiveness as materials for photoelectric conversion and photocatalysis, but also for its inexpensiveness, easy production, photochemical and biological stability, and innocuity to the environment and human beings [1–3]. However, TiO_2 has a wide energy band gap of 3.2 eV so that it can be excited only by the ultraviolet light which is only about 4–6% of the solar spectrum. So, TiO_2 nanoparticles cannot efficiently utilize the solar energy. In addition, the high recombining probability of electrons and holes photogenerated in TiO_2 would decrease its photocatalytic activity. All these drawbacks limit its application especially in the large-scale industry. To solve the above problems, many methods have been applied to extend the light absorption of TiO_2 into the visible region and increase its photocatalytic activity, as for instance transition metals ion doping [4–7], non-metals ion doping (including doping of nitrogen [8–12], carbon [13–16], sulfur [17] and iodine [18, 19]), ion implantation [20], and photosensitization [21, 22]. The photosensitization is one of most important modification techniques for improving the photocatalytic activity of TiO_2, in which the usual photosensitizers are the dyes and conducting polymers with the conjugated structure.

In recent years, conducting polymers (e.g., polyaniline, polypyrrole, and polythiophene) have aroused great interest to the researchers because of their unique electrical and optical properties [23, 24], such as high absorption coefficients, efficient electron donors and good electron transporters in the visible light radiation, high mobility of charge carriers, and excellent stability [25]. As a traditional conducting polymer, polyaniline has been studied in the modification of TiO_2 widely [26–29] for improving the photocatalytic activity of TiO_2. As another common conducting polymer, polypyrrole (PPy) has higher conductivity than polyaniline [30]. The conjugated structure and perfect conductivity of PPy can be useful to electron transfer during the photoaction. Kwon et al. prepared various polypyrrole/titania hybrids as the photovoltaic materials using different synthetic methods, and observed that photoelectric conversion efficiencies increased in

Q. Luo · X. Li · D. Wang (✉) · Y. Wang · J. An
School of Sciences, Hebei University of Science and Technology, 050018 Shijiazhuang, People's Republic of China
e-mail: dswang06@126.com

proportion to the polypyrrole content of the hybrid composites [31]. Melo et al. prepared conducting polypyrrole blends gas sensors [32]. But so far, few studies have been carried out on the photocatalytic activity of TiO_2 modified by PPy except that the photocatalytic activity of PPy–TiO_2 nanocomposites under sunlight was studied by our group [33].

In this article, a series of PPy/TiO_2 nanocomposites were prepared by 'in-situ' deposition oxidative polymerization of pyrrole, and the effects of polymerization conditions on their photocatalytic activities were evaluated by photodegradation of methyl orange aqueous solution under visible and UV light. PPy/TiO_2 nanocomposites were characterized by TEM, XPS, FT-IR, and UV–Vis spectra. The reasons for improving the photocatalytic activity of PPy/TiO_2 nanocomposites were also discussed.

Experimental

Reagents and materials

Pyrrole (Tianjin Chemical Works, China) was used after distillation at reduced pressure. Methyl orange, ferric chloride, tetrabutyl titanate, and hydrochloric acid (Tianjin Chemical Reagents Company) were of AR grade and used without further purification. Absolute ethanol and acetic acid (Beijing Chemical Reagents Company) were used as received. The water was deionized water in this study.

Preparation of TiO_2 nanoparticles

Nanoparticulate TiO_2 (mostly anatase) was prepared in our laboratory by sol–gel hydrolysis and condensation of ethanol solutions of tetrabutyl titanate as follows. Tetrabutyl titanate and acetic acid were added into absolute ethanol under continuously stirring condition. Deionized water, absolute ethanol, and acetic acid were mixed together to inject dropwise into the above solution for 30 min under magnetic stirring. The obtained mixture was stirred for another 30 min and aged for 24 h at room temperature and then dried in an oven at 100 °C for 36 h. After grinded, the final gels were heat-treated in a furnace at 500 °C for 3 h.

Preparation of PPy/TiO_2 nanocomposites

PPy/TiO_2 nanocomposites were prepared according to the reported procedure [33]. The as-prepared TiO_2 nanoparticles (2.0 g) were suspended in HCl aqueous solution (1.5 mol/L, 100 mL) and sonicated for 30 min. Then pyrrole (the molar ratio of TiO_2 to pyrrole in the polymerization system was from 60:1 to 140:1) was injected into the above suspension at certain temperature (0, 15, 25, 35, and 45 °C) with constant stirring. After that, ferric chloride dissolved into 1.5 mol/L hydrochloric acid aqueous solution was added to the above mixture by dropwise. The resulting mixture reacted at constant temperature bath for the designed time (2, 4, 6, 8, and 10 h). Afterward, the reaction mixture was filtered, the precipitate was washed with hydrochloric acid solution, and a large amount of deionized water, respectively. Finally, the product was dried at 100 °C until its mass reached the constant. According to this method, a series of PPy/TiO_2 samples were synthesized and labeled as PPy/TiO_2 (1:X), where 1:X is the molar ratio of pyrrole monomer to TiO_2.

Measurements of photocatalytic activities

Photocatalytic activities of the samples were evaluated in terms of the photodegradation of methyl orange (MO) aqueous solution under UV or visible light illumination. A 20 W UV lamp (Beijing Lighting Research Institute, with peak emission at $\lambda = 254$ nm) and a 300 W tungsten halogen lamp (PHILIPS, equipped with a 400 nm cut-off filter) were used as UV light and visible light source, respectively. The distance between the lamp and the surface of suspension was about 10 cm. Circulating water was used to cool the suspensions for visible light photocatalytic reactions. PPy/TiO_2 nanocomposites (0.4 g) were suspended into 10 mg L^{-1} MO aqueous solution (400 mL) and sonicated for 30 min to disperse the nanoparticles well. Then the suspension containing MO and photocatalyst was magnetically stirred in a dark condition for 60 min until an adsorption–desorption equilibrium was established. After that, the suspension was irradiated under UV or visible light. At the given time intervals, a few milliliters of the suspension were taken out and separated by high speed centrifugation. The concentration of clarified solution was analyzed by measuring the absorbance of MO at a wave length of 464 nm with a 723 spectrometer. The degradation rate (D, %) could be calculated as the following equation:

$$D = (c_0 - c_t)/c_0 \times 100\% \quad (1)$$

Where, c_0 and c_t are the concentrations of MO solution before and after irradiation, respectively.

Characterization

Fourier transform infrared spectra (FT-IR) of the samples were recorded on spectrometer (SHIMADZU) in the range 400–4000 cm^{-1}. Measurements were performed in the transmission mode in spectroscopic grade KBr pellets for all the powders. Transmission electron microscopy (TEM) images were taken on a tecnai G2 F20 transmission electron microscopy, whereby the samples were dispersed on a carbon-coated copper grid. The x-ray diffraction (XRD)

patterns of both neat TiO_2 and PPy/TiO_2 were obtained in the scanning range of $2\theta = 10$–$90°$ on a Rigaku D/MAX-2500 diffractometer (Rigaku Co., JAPAN) operated at 40 kV and 100 mA using Cu Kα radiation ($\lambda = 0.15406$ nm). The UV–visible diffuse reflectance spectra of the catalysts were measured between 200 and 800 nm using a Varian Cary 100 Scan UV–visible system equipped with an integrating sphere attachment (USRS-99-010) as a reflectance standard. X-ray photoelectron spectrometer (XPS) was carried out on a Perkin Elmer PHI1600 ESCA system with an Mg Ka x-ray source. In the data analysis, the binding energy of core level C1s was set at 284.8 eV to compensate for surface-charging effects. Specific surface area of nanopaticles was calculated using BET method, and adsorption–desorption isotherms of nitrogen at 77 K were measured on the NOVA2000 adsorption instrument (Quantachrome Instruments Co., USA).

Results and discussion

Morphology of TiO_2 nanoparticles and PPy/TiO_2 nanocomposites

Figure 1 shows the transmission electron microscope images of neat TiO_2 nanoparticles and PPy/TiO_2 (1:100) nanocomposites. It can be found that the morphology and sizes of the nanocomposites (Fig. 1b) do not differ much from those of neat TiO_2 (Fig. 1a), while the aggregation of PPy/TiO_2 nanocomposites is less than that of neat TiO_2, indicating that modification of PPy can alleviate the aggregation of TiO_2 nanoparticles. The typical HRTEM image of PPy/TiO_2 (1:100) (inset of Fig. 1b) reveals that the thickness of PPy layer adsorbed on TiO_2 surface is about 0.7 nm. Based on the fold-line frame structure of PPy molecules and the size of pyrrole structure, we can infer that PPy on TiO_2 surface might exist with the monomolecular layer, which is similar to that described in the literature [34]. The XRD patterns of neat TiO_2 nanoparticles and PPy/TiO_2 (1:100) nanocomposites are shown in Fig. 2. It can be concluded that anatase diffraction peak at 25.3, 37.8, and 48.1° appeared which attributed to the 101, 004, and 200 reflection, respectively, indicating the as-prepared TiO_2 is anatase phase. The mean sizes of TiO_2 nanoparticles and PPy/TiO_2 nanocomposites calculated from Scherrer's formula, are 14.6 and 15.5 nm, respectively. In addition, the specific surface area (82.6 $m^2\ g^{-1}$) of PPy/TiO_2 (1:100) nanocomposites, determined from the adsorption isotherm of nitrogen at 77 K, is obviously larger than that (69.3 $m^2\ g^{-1}$) of neat TiO_2, further confirming that PPy deposited on the surface of TiO_2 nanoparticles can improve the dispersity of PPy/TiO_2 nanocomposites. The reason for the dispersity improvement of TiO_2 nanoparticles may be that the molecules of doped PPy possess positive charges, leading PPy/TiO_2 nanoparticles to repel each other and alleviate their aggregation.

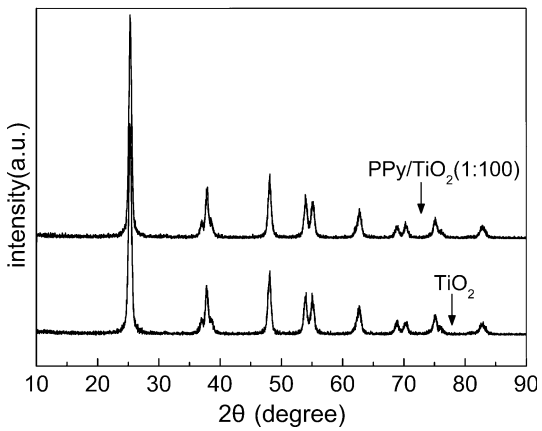

Fig. 2 XRD patterns of neat TiO_2 and PPy/TiO_2 (1:100)

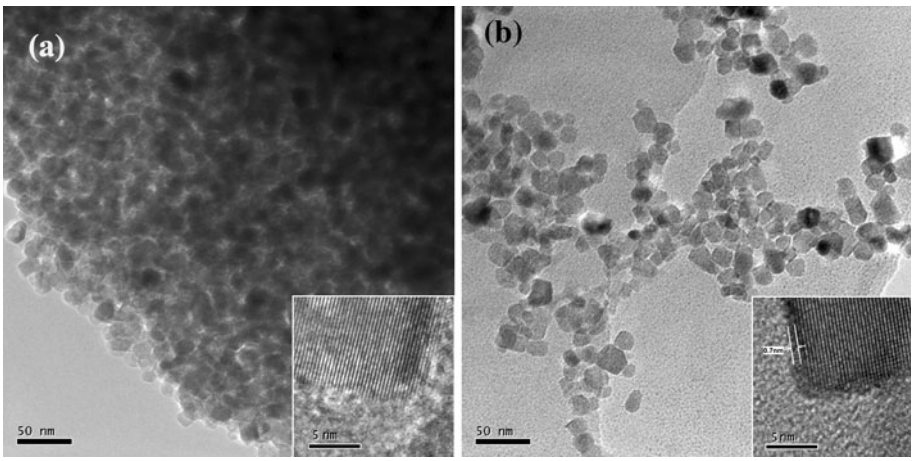

Fig. 1 TEM images of **a** neat TiO_2 and **b** PPy/TiO_2 (1:100)

Light absorption of PPy/TiO_2 nanocomposites

Figure 3 displays the UV–visible diffuse reflectance spectra of PPy/TiO_2 (1:100) nanocomposites prepared at different polymerization time. It can be clearly seen that the absorbance of PPy/TiO_2 is enhanced within the whole range of visible light. With prolonging polymerization time, the visible light absorbance of PPy/TiO_2 increases, which might be associated with PPy content on the surface of TiO_2 nanoparticles. The results reveal that PPy can facilitate nanocomposites to absorb more visible light and generate more electron–hole pairs, which could result in the higher photocatalytic activities of TiO_2 nanoparticles.

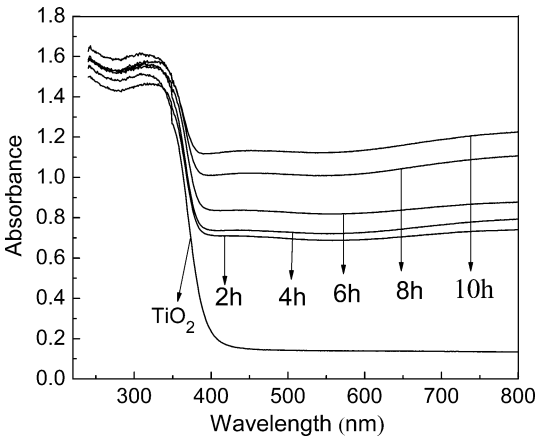

Fig. 3 UV–Vis diffuse reflectance spectra of PPy/TiO_2 (1:100) nanocomposites prepared at different polymerization time

Interaction between PPy and TiO_2

According to the XPS survey spectra (Fig. 4) of PPy/TiO_2 (1:100), the nanocomposite contains the elements of Ti, O, C, and N. The binding energies for C1s, O1s, Ti2p, and N1s are 284.8, 529.8, 458.5, and 399.44 eV, respectively. To investigate the polypyrrole states in the photocatalyst, we measured C1s, O1s core levels. The peaks at binding energies of 284.87 and 286.66 eV indicate the presence of C in polypyrrole. The peak of 288.75 eV indicates the presence of C–O bond. The signal of O1s at 529.8 eV confirms the Ti–O bond in TiO_2, and the other peak at 531.9 eV is attributed to the presence of H-bonds between O in TiO_2 and H in the N–H of polypyrrole. It can be inferred that the H-bonds lead to the tight combination between TiO_2 and PPy.

Figure 5 compares the FT-IR spectra of neat TiO_2, PPy doped by HCl and PPy/TiO_2 sample. The main characteristic peaks of PPy are assigned as follows: the bands at 3422 and 1625 cm^{-1} are attributable to N–H stretching mode and bending mode, respectively. C=C and C–N stretching modes for the polypyrrole rings occur at 1540 and 1454 cm^{-1}, respectively. The bands at 1294, 1170, and 1040 cm^{-1} are also attributed to stretching mode for polypyrrole. The spectrum of neat TiO_2 has one major band at about 500 cm^{-1}. Many characteristic peaks of PPy

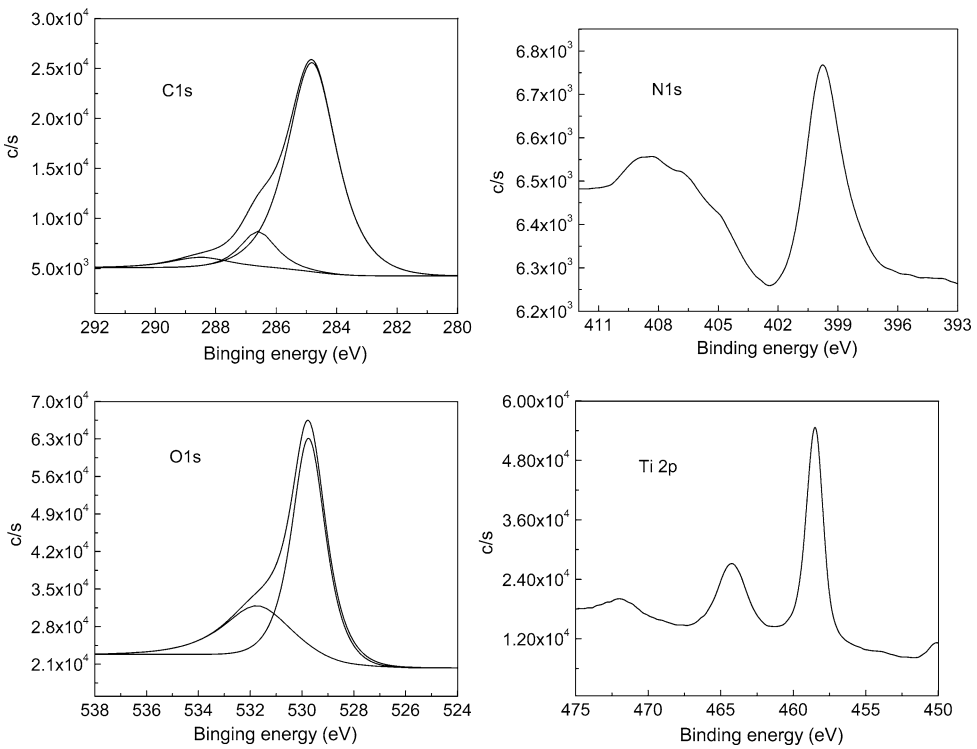

Fig. 4 XPS spectra of C1s, O1s, Ti2p, and N1s in PPy/TiO_2 (1:100) nanocomposites

disappear in the spectrum of the PPy/TiO_2 (1:100) nanocomposites due to the small content of PPy in nanocomposites. PPy/TiO_2 (1:5) nanocomposites were prepared by the same method in order to explain the interaction between PPy and TiO_2. The bands at 3432, 1634, 1559, 1465, 1303, and 500 cm^{-1} appear in the spectrum of PPy/TiO_2 (1:5) nanocomposites, which can be concluded that the nanocomposites are composed of PPy and TiO_2. Compared with the spectrum of PPy, the characteristic peaks of PPy in nanocomposites shift to higher wave number, indicating that a strong interaction exists at the interface between TiO_2 and PPy.

Photocatalytic activities of PPy/TiO_2 nanocomposites under UV and visible light

A series of samples of PPy/TiO_2 nanocomposites were prepared in different polymerization conditions, and the effects of polymerization conditions on photocatalytic activities of the samples were investigated by MO degradation under UV or visible light illumination. The results were showed in Figs. 6, 7, and 8.

Figure 6 shows that the degradation of MO can be described by first-order reaction in the presence of neat TiO_2 or PPy/TiO_2 nanocomposites with different molar ratios of pyrrole monomer to TiO_2 under UV or visible light irradiation, and the kinetics plots are shown by apparent first-order linear transform $\ln(c_0/c) = k_{app}\, t$. The photocatalytic activities of neat TiO_2 and PPy/TiO_2 catalysts can be evaluated by comparing the apparent rate constants (k_{app}) listed in Table 1. It is found that PPy/TiO_2 nanocomposites have higher photocatalytic activities than neat TiO_2. The introduction of a small amount of PPy to TiO_2 nanoparticles enhances the photocatalytic activities under UV and visible light. With the increase of the molar ratio of pyrrole to TiO_2 from 1:140 to 1:60, the degradation rate of MO increases and then decreases, the highest degradation rate occurs at the molar ratio of 1:100.

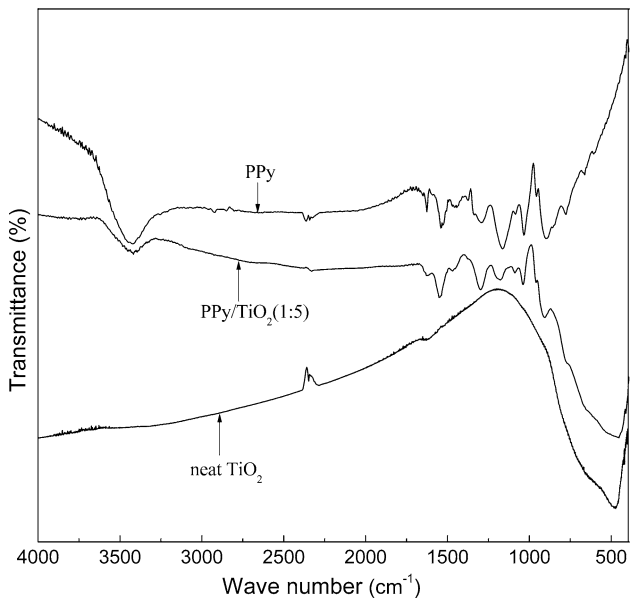

Fig. 5 FT-IR spectra of TiO_2, PPy doped by HCl, and PPy/TiO_2 (1:5) nanocomposites

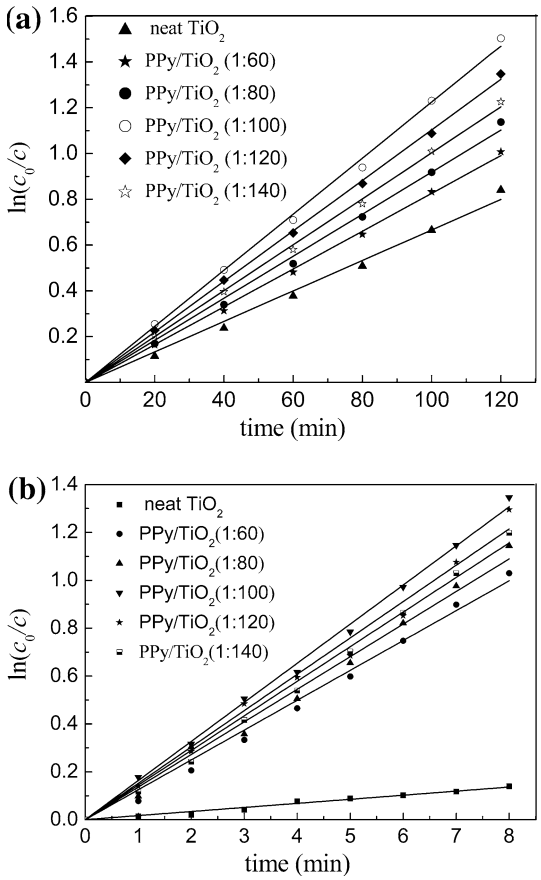

Fig. 6 Apparent first-order linear transform $\ln(c_0/c)$ via time for neat TiO_2 and PPy/TiO_2 nanocomposites with different molar ratios of pyrrole to TiO_2 under **a** UV light illumination and **b** visible light irradiation

The higher photocatalytic activities of PPy/TiO_2 nanocomposites compared with neat TiO_2 under UV light can be interpreted by the two aspects as follows. First, the introduction of a little of PPy to surface of TiO_2 nanoparticles can decrease the aggregation of TiO_2 nanoparticles and increase the specific surface area due to repelling force of the nanoparticles from the doped PPy with the positive charges. PPy/TiO_2 nanoparticles with larger specific surface area have higher absorption of MO, which can lead to faster degradation rate under UV light. Second, a strong interaction exists at the interface between TiO_2 and PPy, and the conjugated structure and perfect conductivity of PPy can easily transfer the electrons generated in TiO_2 nanoparticles under UV light, so the recombining

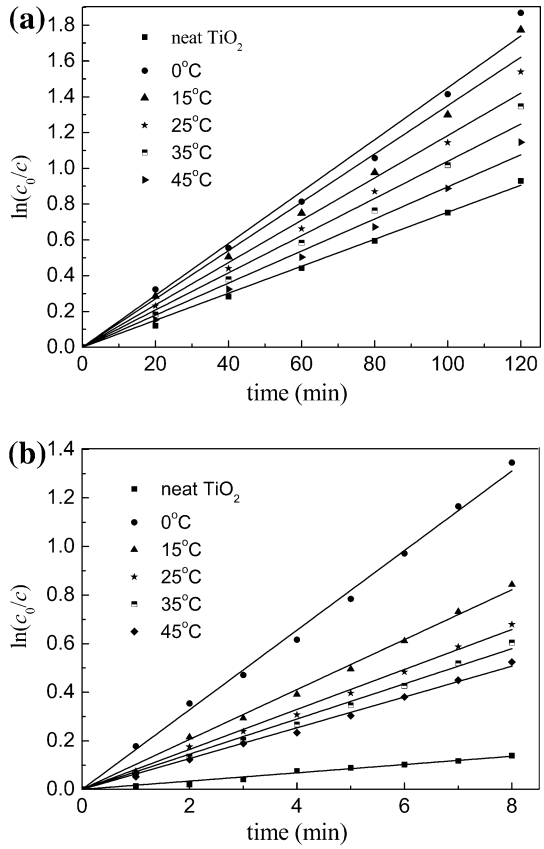

Fig. 7 Relationship between $\ln(c_0/c)$ and time for MO photodegradation catalyzed by PPy/TiO_2 nanocomposites prepared at different polymerization temperatures under **a** UV light illumination and **b** visible light irradiation

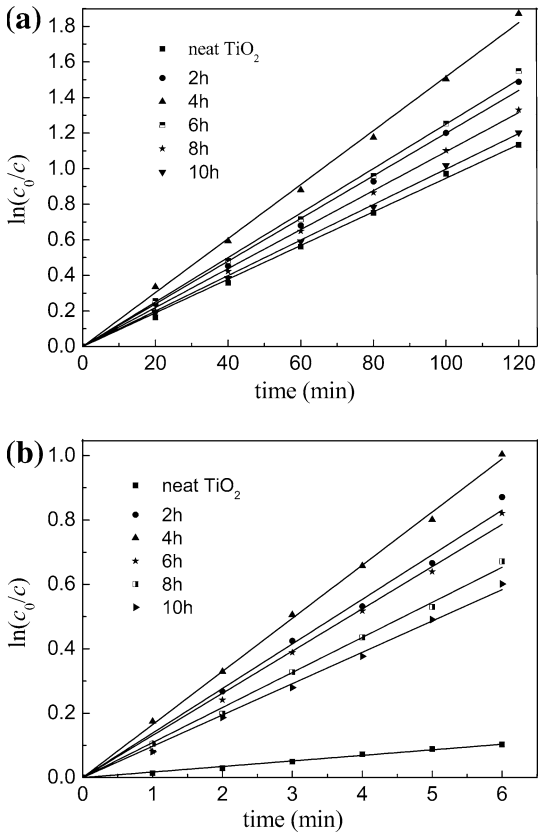

Fig. 8 Relationship between $\ln(c_0/c)$ and time during MO photodegradation in the presence of PPy/TiO_2 nanocomposites prepared at different polymerization time under **a** UV light illumination and **b** visible light irradiation

probability of photogenerated electrons and holes decreases and their separating probability increases, which favors the improvement of photocatalytic activity of PPy/TiO_2 nanoparticles under UV light. Simultaneously, except for the above two aspects which can also favor the photocatalytic activities of PPy/TiO_2 nanocomposites under visible light, the third reason is that absorbance spectra of PPy/TiO_2 nanocomposites presented in Fig. 3 would favor the photocatalytic activities of PPy/TiO_2 nanocomposites under visible light instead of UV light. PPy/TiO_2 nanocomposites show stronger absorbance in the whole visible light range. When PPy/TiO_2 nanocomposites are illuminated under visible light, PPy can absorb photons and be excited to produce electron–hole pairs. The electrons photogenerated by conducting PPy under visible light can transfer to the conduction band of TiO_2, which can enhance the electron–hole separation and in turn improve the visible light photocatalytic ability of PPy/TiO_2 nanocomposites. Therefore, PPy/TiO_2 nanocomposites have significantly higher photocatalytic activity than neat TiO_2 nanoparticles under visible light.

With increasing pyrrole concentration in the polymerization system, the PPy content on the surface of PPy/TiO_2 nanocomposites increases, which favors the increment of the specific surface area of the nanocomposites, separating probability of electrons and holes photogenerated on nanocomposites, and the absorbance of nanocomposites in visible light region. So, the photocatalytic activity of the nanocomposites under UV or visible light irradiation increases. When PPy layer on the nanocomposite surface is thicker than that of the monomolecular layer, more PPy content cannot obviously increase the specific surface area of TiO_2 nanoparticles because of the repelling force not greatly increasing, and not obviously decrease the recombining probability of photogenerated electrons and holes. However, too more PPy content may decrease UV light absorbance to excite TiO_2, and disfavor the electrons photogenerated by conducting PPy under visible light to transfer to the conduction band of TiO_2 because the most easily excited PPy might not tightly touch with TiO_2. So, further increasing pyrrole concentration in the polymerization system can decrease the photocatalytic activity of the nanocomposites under UV or visible light irradiation. For the PPy/TiO_2 (1:100) nanocomposites, all the abovementioned factors favor the photocatalytic activity due to the monomolecular layer of PPy on the surface of TiO_2, so

Table 1 Apparent rate constants (k_{app}) of MO photodegradation catalyzed by neat TiO_2 and PPy/TiO_2 nanocomposites prepared with different molar ratios of pyrrole to TiO_2 and linear regression coefficients from a plot of $\ln(c_0/c) = k_{app}t$

n(Py):n(TiO_2)	Under UV light illumination		Under visible light irradiation	
	k_{app} (min^{-1})	R	k_{app} (h^{-1})	R
Neat TiO_2	0.00707	0.9976	0.0170	0.9930
1:60	0.00826	0.9995	0.125	0.9965
1:80	0.00976	0.9989	0.136	0.9952
1:100	0.0130	0.9989	0.163	0.9990
1:120	0.0117	0.9996	0.152	0.9959
1:140	0.0106	0.9994	0.145	0.9981

Table 2 Apparent rate constants (k_{app}) and linear regression coefficients from a plot of $\ln(c_0/c) = k_{app}t$ of MO photodegradation catalyzed by PPy/TiO_2 nanocomposites prepared at different polymerization temperatures

Polymerization temperature (°C)	Under UV light illumination		Under visible light irradiation	
	k_{app} (min^{-1})	R	k_{app} (h^{-1})	R
0	0.0145	0.9949	0.164	0.9989
15	0.0135	0.9926	0.103	0.9978
25	0.0118	0.9943	0.0823	0.9968
35	0.0104	0.9946	0.0724	0.9979
45	0.00896	0.9960	0.0634	0.9985
Neat TiO_2	0.00755	0.9988	0.0172	0.9936

the photocatalytic activity is highest under UV or visible light irradiation.

The effects of polymerization temperatures on degradation of MO under UV or visible light irradiation were shown in Fig. 7. The degradation rate constants (k_{app}) were displayed in Table 2. It is found that photocatalytic activity of PPy/TiO_2 nanocomposites decreases with the increase of polymerization temperature under both UV light and visible light irradiation. This is likely related to PPy structure on the surface of TiO_2. At lower temperatures the polymerization rate of pyrrole is lower, and a higher degree of structural regularity can be easily obtained during the formation of PPy chains, which will be favorable to the photocatalytic activity. With the increase of polymerization temperature, oxidative polymerization rate may be so fast that the conjugated degree of polymer chain decreases, resulting in lower photocatalytic activity.

Figure 8 displays MO photodegradation catalyzed by neat TiO_2 and PPy/TiO_2 nanocomposites prepared at different polymerization time. The degradation rate constants (k_{app}) were listed in Table 3. It can be seen that the photocatalytic activities of PPy/TiO_2 nanocomposites increase and then decrease with the increase of polymerization time from 2 to 10 h, the highest degradation rate occurs at 4 h. The experimental result can be explained as follows. With prolonging the polymerization time, the content of PPy on TiO_2 surface increases gradually, and the absorbance of TiO_2/PPy nanocomposites in the visible light region also increases as shown in Fig. 3, which can favor the photocatalytic activities of TiO_2/PPy samples. However, further prolonging the polymerization time might lead to other side reactions such as the overoxidation of PPy, which disfavors the photocatalytic activities of PPy/TiO_2 nanocomposites.

Table 3 Apparent rate constants (k_{app}) and linear regression coefficients from a plot of $\ln(c_0/c) = k_{app}t$ of MO photodegradation in the presence of PPy/TiO_2 nanocomposites prepared at different polymerization time

Polymerization time/h	UV light illumination		Visible light illumination	
	k_{app} (min^{-1})	R	k_{app} (h^{-1})	R
2	0.0120	0.9987	0.138	0.9970
4	0.0152	0.9991	0.165	0.9995
6	0.0125	0.9989	0.131	0.9967
8	0.0109	0.9996	0.109	0.9990
10	0.00998	0.9997	0.0973	0.9987
Neat TiO_2	0.00947	0.9994	0.0172	0.9980

Photocatalytic stabilities of PPy/TiO_2 nanocomposites under UV and visible light

The photocatalytic stabilities of PPy/TiO_2 nanocomposites under UV and visible light were performed with the concentration of MO (10 mg L^{-1}) and catalyst dosage (1 g L^{-1}) for each cycling run. The regeneration of PPy/TiO_2 was done by filtrating the suspension to remove the bulk solution and drying the photocatalysts at 60 °C for 24 h. The regenerated photocatalysts were reused in the next cycle. The results displayed in Fig. 9 show that the degradation rate of MO is still about 70% of that of the first cycling run after five successive cycles under UV and visible light irradiation, indicating that the phtotocatalytic

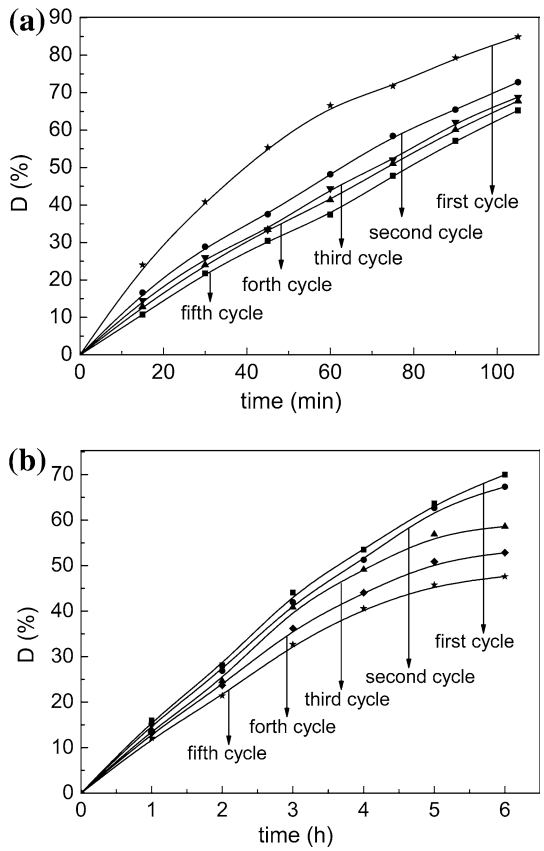

Fig. 9 The photocatalytic experiments of PPy/TiO_2 (1:100) nanocomposites for five cycles under **a** UV light illumination and **b** visible light irradiation

stabilities of PPy/TiO_2 nanocomposites are excellent. The slight decrease of photocatalytic activity after each cycle may be due to the aggregation of nanoparticles during the photocatalytic degradation process.

Conclusions

PPy/TiO_2 nanocomposites were prepared by 'in situ' chemical oxidative polymerization of pyrrole in the TiO_2 suspension. The degradation of MO in aqueous solution was carried out to evaluate the photocatalytic activity. It was found that PPy/TiO_2 nanocomposites showed significantly higher photocatalytic activities than neat TiO_2 under visible and UV light irradiation, and the highest photocatalytic activity of PPy/TiO_2 nanocomposites was obtained when the molar ratio of pyrrole monomer to TiO_2 was 1:100, the polymerization temperature was 0 °C, and the polymerization time was 4 h. TEM images and BET-specific surface areas showed that PPy could enhance the dispersity of TiO_2 nanoparticles efficiently. UV–Vis diffuse reflectance spectra confirmed that the PPy/TiO_2 nanocomposites could absorb more photons under visible light irradiation. XPS and FT-IR analyses suggested that a strong interaction existed at the interface between PPy and TiO_2 in the nanocomposites. PPy modification could be an efficient method to improve the visible light photocatalytic activity of TiO_2 photocatalyst.

Acknowledgement The authors are grateful for the financial support by the Nature Science Foundation of Hebei Province (Grant no. B2010000846).

References

1. Hashimoto K, Irie H, Fujishima A (2005) Jpn J Appl Phys 44:8269
2. Legrini O, Oliveros E, Braun AM (1993) Chem Rev 93:671
3. Linsebigler AL, Lu GQ, Yates JT (1995) Chem Rev 95:735
4. Yu J, Xiang Q, Zhou M (2009) Appl Catal B Environ 90:595
5. Ghasemia S, Rahimnejada S, Rahman SS, Rohanib S (2009) J Hazard Mater 172:1573
6. Cao Y, Tan H, Shi T, Tang T, Li J (2008) J Chem Technol Biotechnol 83:546
7. Cheng P, Deng C, Gu M, Shangguan W (2007) J Mater Sci 42:9239. doi:10.1007/s10853-007-1902-5
8. Asahi R, Morikawa T, Ohwaki T, Aoki K, Taga Y (2001) Science 293:269
9. Tessier F, Zollfrank C, Travitzky N, Windsheimer H, Merdrignac-Conanec O, Rocherulle′ J, Greil P (2009) J Mater Sci 44:6110. doi:10.1007/s10853-009-3845-5
10. Jo WK, Kim JT (2009) J Hazard Mater 164:360
11. Kisch H, Sakthivel S, Janczarek M, Mitoraj D (2007) J Phys Chem C 111:11445
12. Xing M, Zhang J, Chen F (2009) Appl Catal B Environ 89:563
13. Chen C, Long M, Zeng H, Cai W, Zhou B, Zhang J, Wu Y, Ding D, Wu D (2009) J Mol Catal A Chem 314:35
14. Xu C, Killmeyer R, Gray ML, Khan SUM (2006) Appl Catal B Environ 64:312
15. Kang IC, Zhang Q, Yin S, Sato T, Saito F (2008) Appl Catal B Environ 80:81
16. Dong F, Wang H, Wu Z (2009) J Phys Chem C 113:16717
17. Hamadanian M, Reisi-Vanani A, Majedi A (2009) Mater Chem Phys 116:376
18. Liu G, Chen Z, Dong C, Zhao Y, Li F, Lu GQ, Cheng HM (2006) J Phys Chem B 110:20823
19. Song S, Tu J, He Z, Hong F, Liu W, Chen J (2010) Appl Catal A Gen 378:169
20. Lam RCW, Leung MKH, Leung DYC, Vrijmoed LLP, Yam WC, Ng SP (2007) Solar Energy Mater Solar Cells 91:54
21. Kathiravan A, Renganathan R (2009) J Colloid Interf Sci 331:401
22. Neves MC, Nogueira JMF, Trindade T, Mendonca MH, Pereira MI, Monteiro OC (2009) J Photochem Photobiol A Chem 204:168
23. Karim MR, Lim KT, Lee CJ, Bhuiyan MTI, Kim HJ, Park LS, Lee MS (2007) J Polym Sci A Polym Chem 45:5741
24. Karim MR, Lee HW, Cheong IW, Park SM, Oh W, Yeum JH (2010) Polym Compos 31:83
25. Liang H, Li X (2009) Appl Catal B Environ 86:8
26. Salem MA, Al-Ghonemiy AF, Zaki AB (2009) Appl Catal B Environ 91:59
27. Yavuz AG, Gők A (2007) Synth Met 157:235
28. Li XY, Wang DS, Cheng GX, Luo QZ, An J, Wang YH (2008) Appl Catal B Environ 81:267
29. Min S, Wang F, Han Y (2007) J Mater Sci 42:9966. doi:10.1007/s10853-007-2074-z

30. Guimarda NK, Gomezb N, Schmidt CE (2007) Prog Polym Sci 32:876
31. Kwon JD, Kim PH, Keum JH, Kim JS (2004) Solar Energ Mater Solar Cells 83:311
32. Melo CP, Neto BB, Lima EG, Lira LFB, Souza JEG (2005) Sensor Actuator B 109:348
33. Wang D, Wang Y, Li X, Luo Q, An J, Yue J (2008) Catal Commun 9:1162
34. Zhang H, Zong R, Zhao J, Zhu Y (2008) Environ Sci Technol 42:3803